ISSN 1063-7834, Physics of the Solid State, 2014, Vol. 56, No. 12, pp. 2380–2386. © Pleiades Publishing, Ltd., 2014.
Original Russian Text © D.M. Gokhfeld, 2014, published in Fizika Tverdogo Tela, 2014, Vol. 56, No. 12, pp. 2298–2304.

SUPERCONDUCTIVITY

An Extended Critical State Model: Asymmetric Magnetization Loops and Field Dependence of the Critical Current of Superconductors

D. M. Gokhfeld

Kirensky Institute of Physics, Siberian Branch of the Russian Academy of Sciences, Akademgorodok 50–38, Krasnoyarsk, 660036 Russia

e-mail: gokhfeld@iph.krasn.ru

Received June 26, 2014

Abstract—An extended critical state model has been developed. The model has considered the equilibrium magnetization of a surface layer and the magnetization of the central region of a superconducting sample. The magnetic flux distributions in the sample have been calculated. An analytical dependence of the critical current density on the magnetic field with different behaviors in strong and weak fields has been proposed. A relation of the asymmetry of the magnetization loops and the critical current density to the sample size has been established. The model is applicable to the parameterization of magnetization loops of single-crystal and polycrystalline superconductors.

DOI: 10.1134/S1063783414120129

1. INTRODUCTION

Measurement of hysteresis dependences of magnetization is the conventional indirect method for determining the critical current density of a superconductor. The relationship between the critical current density j_c of a superconductor and the hysteresis loop of the magnetization $M(H)$ was obtained in the critical state model [1]. The modified critical state models (see, for example, [2–4]), which take into account the field dependence of the critical current density j_c, successfully describe magnetization loops that are symmetric with respect to the H axis ($M = 0$). However, for many superconducting materials, magnetization loops have a pronounced axial asymmetry with respect to the H axis ($M = 0$). The asymmetry of the dependence $M(H)$ increases with increasing temperature. For example, in high-temperature superconductors (HTSCs), the asymmetry of magnetization loops can manifest itself after the increase in temperature to ~10–30 K [5–7].

The asymmetric magnetization loops were adequately described in the framework of the extended critical state model (ECSM) [8]. In the ECSM, the total magnetization of a sample is the sum of the equilibrium magnetization M_s of the surface layer and the nonequilibrium magnetization M_b of the remaining volume of the sample. In the surface layer, the vortices are not pinned due to the interaction with the screening currents and the surface [9, 10]. The magnetization M_b is described by the critical state model [2] with modified boundary conditions that take into account the magnetization of the surface layer. The asymmetry of the magnetization loop is determined by the fraction of the equilibrium magnetization M_s in the total magnetization of the sample. Asymmetric magnetization loops of different superconductors were successfully described by the ECSM [5, 6]. However, the use of this model is complicated by a large number of fitting parameters with the dimension of field, which cannot be evaluated or tested in other experiments [9]. For promising applications of bulk superconductors [11–13] (levitation, magnets, electric motors, etc.), information about the field dependence of the critical current and about the frozen field is particularly important [14, 15]. In the framework of the model proposed in [8], such data cannot be obtained.

Since 2011, a new ECSM version has been developed [7], in which the magnetization is determined by the field distribution in a sample and the asymmetry of the magnetization loop is related to the depth of the surface layer with equilibrium magnetization. In this paper, we have performed a detailed description of the ECSM, which takes into account the field dependence of the surface layer depth, and presented the algorithm for the calculation and parameterization of magnetization loops. The paper is organized as follows. Section 2 presents the model equations and demonstrates the use of the ECSM for the description of magnetization loops (Subsections 2.1 and 2.2). Subsection 2.3 discusses the determination of the field dependence of the bulk critical current density. Section 3 describes the specific features of the magnetization of heterogeneous and granular superconductors and presents the algorithm for the ECSM description of experimental magnetization loops.

2. THE MODEL

2.1. Basic Equations

We consider a sample in the form of a cylinder with the length significantly larger than the size of the base, so that the demagnetization factor of the sample can be taken as zero. By definition, the magnetization has the form $M(H) = -H + \bar{B}(H)/\mu_0$, where $\bar{B}$ is the averaged flux density (magnetic induction) of the magnetic field inside the sample and μ_0 is the magnetic constant. For an infinitely long cylindrical sample with radius R, which is coaxial with the external magnetic field, the magnetization is determined by the following expression:

$$M(H) = -H + \frac{2}{\mu_0 R^2}\int_0^R rB dr, \qquad (1a)$$

where r is the distance from the cylinder axis. Similarly, for a sample in the form of an infinitely long plate oriented along the field with a small thickness and width $2R$, we can write

$$M(H) = -H + \frac{1}{\mu_0 R}\int_0^R B dr. \qquad (1b)$$

The distribution of the flux density B inside the sample is determined by Ampére's circuital law

$$dB/dr = \pm\mu_0 j_c(B), \qquad (2)$$

where j_c is the local critical current density in the sample. By choosing the appropriate dependence $j_c(B)$ (see Section 3) and integrating equation (1), we can determine the distribution $B(r)$, which depends on the magnetic field H and the magnetization prehistory. Following [16], we introduce the function

$$F(B) = \int_0^B j_{c0}/j_c(B')dB'. \qquad (3)$$

Here, j_{c0} is the value of $j_c(B)$ for $B = 0$. This function allows us to rewrite equation (2) for the numerical solution

$$\pm\mu_0 j_{c0}(R - r) = F(B) - F(\mu_0 H). \qquad (4)$$

Now, we consider the distribution of the flux density B in the cylindrical sample for a specific value of the external field H (Fig. 1). According to the ECSM, the magnetization of the sample first leads to the penetration of the magnetic flux into the surface layer (plot AB in Fig. 1). The field distribution in the surface layer with depth l_s does not depend on the magnetization prehistory. Let B at the depth l_s from the surface be designated as $B_s(H)$. With an increase in the external field H, when the value of $B_s(H)$ becomes larger than zero, the magnetic flux begins to penetrate into the central region of the sample (plot BC). In the external field $H = H_p$, the magnetic flux reaches the center of the sample. Therefore, H_p is the field of the complete penetration of the magnetic flux into the sample. With a further increase in the magnetic field H, the flux density B at the center of the sample increases (point E). When the external field reaches the maximum value H_m, it begins to decrease. As a result, the frozen flux remains in the central region of the sample (plot BDE). The frozen field remains in the sample with a decrease in the field H to zero, which leads to the observed hysteresis dependence $M(H)$. Plot CFG in Fig. 1 corresponds to the frozen field in the sample after the external field reaches the value $-H_m$.

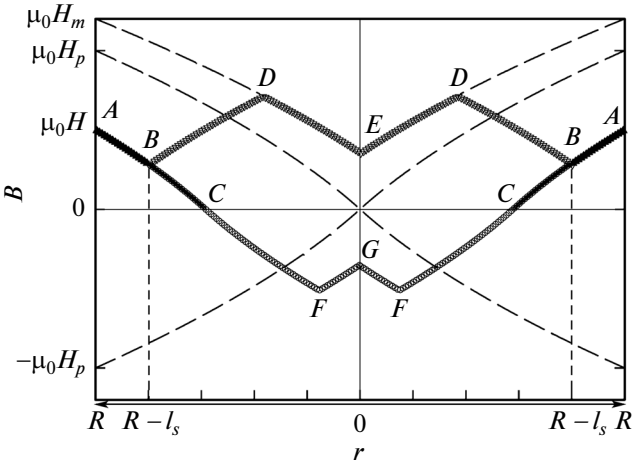

Fig. 1. Distribution of the flux density B in the cylindrical sample. Shown are the penetration of the magnetic flux into the sample (ABC), the frozen flux with variations in the external field from H_m to H ($ABDE$), and the frozen flux with variations in the external field from $-H_m$ to H ($ABCFG$).

For each of the plots in Fig. 1, we can write equation (4) in a more convenient form for further use. For the surface layer with depth l_s, in which the vortices are not pinned, we have

$$F_s(B) - F_s(\mu_0 H) = -\mu_0 j_{s0} R(1 - r/R), \qquad (5a)$$

where $F_s(B)$ is function (3) determined in terms of the surface supercurrent density $j_s(B)$ and j_{s0} is the critical surface current density for $B = 0$. Figure 2 shows the field dependences of the equilibrium magnetization of the surface layer $M_s(H)$, which were calculated according to equations (1) and (5a) (the calculation parameters are presented in Subsection 2.2). Also, Fig. 2 shows the dependence $B_s(H)$. The value of B_s determines the boundary field for the core of the sample (cylinder with radius $R - l_s$).

The magnetization of the central region depends on the magnetization prehistory. The flux density has different profiles in the central region for each of the following magnetization loop branches: (i) the branch of the initial magnetization with an increase in the

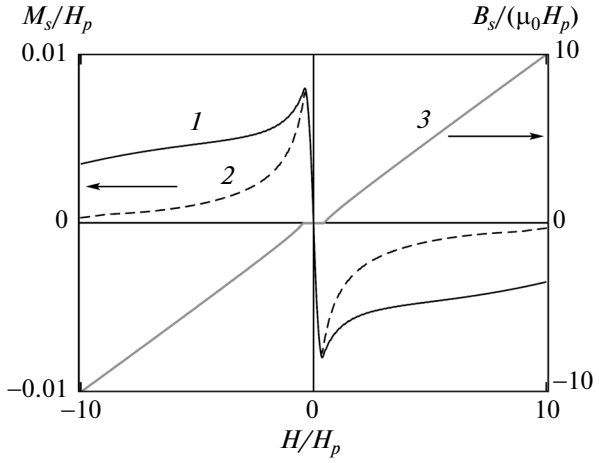

Fig. 2. Magnetic field dependences of the magnetization of the surface layer and the boundary field: (*1*) magnetization of the surface layer in the high-temperature superconductor ($H_{irr} \ll H_{c2}$), (*2*) magnetization of the surface layer in the low-temperature superconductor ($H_{irr} \approx H_{c2}$), and (*3*) boundary field B_s between the surface layer and the core of the sample.

field from zero to H_m (plot *BC* in Fig. 1); (ii) the branch $M^+(H)$ with a decrease in the external field from H_m to zero (plots *BD* and *DE* in Fig. 1); and (iii) the branch $M(H)$ with an increase in H from zero to H_m after the circulation of the external field from zero to $-H_m$ and back to zero (plots *BC*, *CF*, and *FG* in Fig. 1). Next, we write the corresponding equations for the distribution of the flux density B.

Plot *BC*:

$$F(B) - F(B_s(H)) = -\mu_0 j_{c0} R(1 - l_s/R - r/R). \quad (5b)$$

Plot *BD*:

$$F(B) - F(B_s(H)) = \mu_0 j_{c0} R(1 - l_s/R - r/R). \quad (5c)$$

Plot *DE*:

$$F(B) - F(B_s(H_m)) = -\mu_0 j_{c0} R(1 - l_s/R - r/R). \quad (5d)$$

Plot *CF*:

$$F(-B) + F(B_s(H)) = \mu_0 j_{c0} R(1 - l_s/R - r/R). \quad (5e)$$

Plot *FG*:

$$F(-B) - F(B_s(H_m)) = -\mu_0 j_{c0} R(1 - l_s/R - r/R). \quad (5f)$$

The surface supercurrent density j_s depends on the surface barrier. However, focusing on the behavior of the magnetization loop in strong fields, we can ignore the differences between $j_s(B)$ and $j_c(B)$. Further, we will assume $j_s = j_c$. Then, the complete penetration field H_p is determined using the equation

$$R = F(\mu_0 H_p)/(\mu_0 j_{c0}). \quad (6)$$

For the calculation of the total magnetization of the loop, we should choose the dependence $j_c(B)$, which determines the functional dependence of $F(B)$ according to formula (3). It is also necessary to take into account the dependence of the surface layer depth l_s on the external field. The choice of the dependences $j_c(B)$ and $l_s(H)$ will be considered in the next subsection.

2.2. Application

The extended critical state model was used to describe magnetization loops of different superconductors: textured Bi2223 [7], whiskers Bi2212 [17], MgB_2 [18], $Ba_{0.6}K_{0.4}BiO_3$ [19], and *Re*123 [20–22], where *Re* = Y, Nd, or Eu. The magnetization loops of the highly porous Bi2223 [4, 23] were also successfully described by the ECSM [7]. Different dependences $j_c(B)$ were tested in the calculations of the magnetization loops. The dependences $M(H)$ calculated using the Bean model (j_c = const) [1] do not reproduce the shape of experimental magnetization loops. The Anderson–Kim relationship $j_c \sim 1/B$ [24] provides a good description of the dependence $M(H)$ for $H \ll H_{c2}$. The exponential dependence $j_c \sim \exp(-B)$ [2] adequately describes the behavior of the magnetization near H_{c2}. These dependences, usually, do not lead to good agreement between the calculated magnetization loop and the experimental data in strong and weak fields simultaneously [3]. In order to solve this problem, it is necessary to choose such a dependence that will exhibit a different behavior on different scales. Based on the performed fitting, we chose the dependence $j_c(B)$, which is proportional to $1/B$ in weak fields and decreases exponentially in strong fields:

$$j_c(B) = \frac{j_{co}}{\left(\frac{|B|}{B_1}\right)^{\gamma} + \exp\left(\frac{|B|}{B_2}\right)}. \quad (7)$$

Here, B_1 and B_2 are the parameters specifying the characteristic scales and $\gamma \approx 1$. To ensure that the calculated values of j_c tend to zero for $B \geq \mu_0 H_{c2}$, the parameter B_2 must be on the order of $0.1\mu_0 H_{c2}$. Using expression (7), for the function $F(B)$ we obtain the following equation:

$$F(B) = \frac{|B|^{\gamma+1}}{(\gamma+1)B_1} + B_2 \exp\left(\frac{|B|}{B_2}\right) - B_2.$$

The branch $M^+(H)$ of the magnetization loop is determined by the dependence of the surface layer depth l_s on the magnetic field. Let the surface layer depth l_s be equal to the depth of penetration of the magnetic field λ [10, 25]. It should be noted that, in weak fields, the surface layer depth l_s is determined by the ratio of the external field H to the flux density

inside the sample $\bar{B}$ [9], so that the values of l_s can be larger than λ for $\mu_0 H/\bar{B} > 1$ and less than λ for $\mu_0 H/\bar{B} < 1$. In conventional superconductors, the dependence $\lambda(H)$, which is associated with the destruction of Cooper pairs by the magnetic field, is determined by the following expression [26]:

$$\lambda(H) = \lambda_0/(1 - H/H_{c2})^{0.5}. \quad (8)$$

Here, λ_0 is the field penetration depth λ for $H = 0$ and H_{c2} is the second critical field of the superconductor. When the values of the function $l_s(H)$ exceed R, the dependence $M(H)$ is reversible. In conventional superconductors, this condition is satisfied near H_{c2}. For HTSCs, expression (8) is not satisfied [27]. Actually, in HTSCs, the magnetization loop becomes reversible when the magnetic field H exceeds the irreversibility field H_{irr} and $H_{irr} \ll H_{c2}$ [28]. For simplicity, the behavior of the dependence $l_s(H)$ for HTSCs will be described using the linear relationship

$$l_s(H) = l_{s0} + (R - l_{s0})H/H_{irr}, \quad (9)$$

where $l_{s0} \approx \lambda_0$ is the value of l_s for $H = 0$.

Equations (5)–(9) allow us to find the distributions of the flux density B for any value of H depending on the magnetization reversal prehistory. The magnetization loops are calculated according to formula (1) with the obtained distributions of B as functions of r. For "classical" low-temperature superconductors (LTSCs), the dependences $M(H)$ are calculated using expression (8), whereas for HTSCs and "nonclassical" superconductors, it is appropriate to use relationship (9). For $H = 0$, the width of magnetization loops along the M axis and their asymmetry with respect to the H axis are determined by the parameters $P_w = j_{c0}R$ and $P_a = l_{s0}/R$, respectively.

Examples of the dependences $M(H)$ calculated with arbitrary parameters P_w, B_1, B_2, and γ and different values of P_a (from 0 to 1) are shown in Figs. 3a and 3b. Figure 3a depicts the plot of the magnetization loop of the LTSC, which was calculated using expression (8) for $H_{c2} = 20H_p$. The magnetization loops calculated for the HTSC according to relationship (9) for $H_{irr} = 10H_p$ are shown in Fig. 3b. The axes in Figs. 3a and 3b are normalized to the field H_p, and the field quantities are also expressed in terms of H_p. The parameters used in the calculation are as follows: $P_w = F(\mu_0 H_p)/\mu_0$, $B_1 = \mu_0 H_p$, and $B_2 = 2\mu_0 H_p$ for the LTSC and $B_2 = 20\mu_0 H_p$ for HTSC, $\gamma = 1$. Figure 3b also shows the symmetric magnetization loop of the HTSC, which was calculated with the same parameters but for $H_{irr} = 200H_p$.

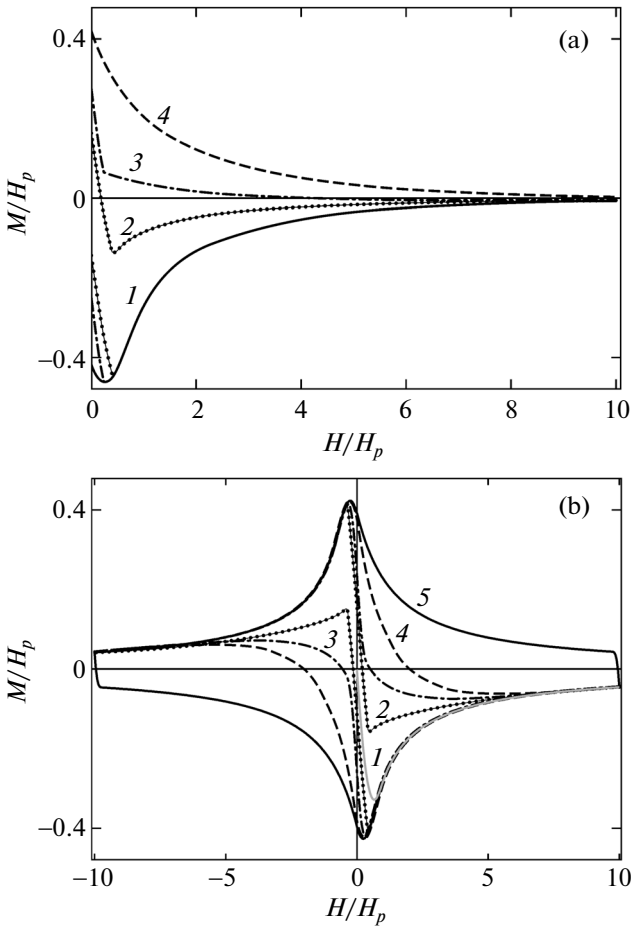

Fig. 3. (a) Plot of magnetization loops of the low-temperature superconductor ($H_{irr} \approx H_{c2}$) according to the ECSM calculation: (*1*) plot of the initial magnetization, which coincides with the branch $M^+(H)$ for $P_a = 1$; (*2*) branch $M^+(H)$ for $P_a = 0.3$; (*3*) branch $M^+(H)$ for $P_a = 0.15$; and (*4*) branch $M^+(H)$ for $P_a = 0$. (b) Magnetization loops of the high-temperature superconductor ($H_{irr} \ll H_{c2}$) according to the ECSM calculation: (*1*) plot of the initial magnetization, which coincides with the branch $M^+(H)$ for $P_a = 1$; (*2*) branch $M^+(H)$ for $P_a = 0.3$; (*3*) branch $M^+(H)$ for $P_a = 0.15$; (*4*) branch $M^+(H)$ for $P_a = 0$; and (*5*) branch $M^+(H)$ for $P_a = 0$ and $H_{irr} \gg H_m$.

2.3. Critical Current Density

The determination of the critical current density and its field dependence is the main task of the analysis of the magnetization loops. The critical state model [1] gives a simple formula for determining the averaged (over the sample) critical current density from magnetic measurements:

for a long cylinder,

$$J_{cm}(H) = 3\Delta M(H)/(2R), \quad (10a)$$

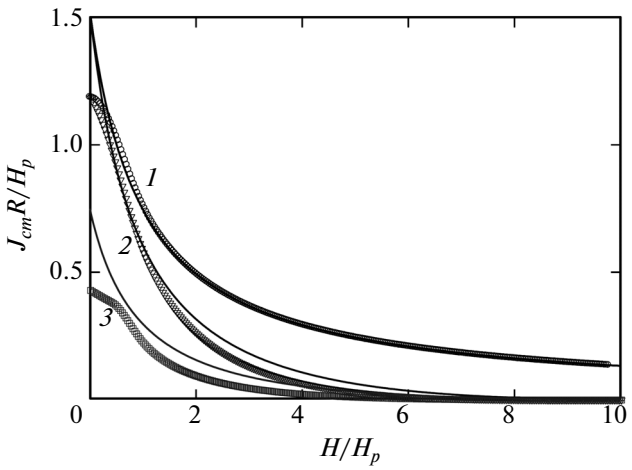

Fig. 4. Dependences $J_{cm}(H)$. Curves were obtained using formulas (10a) (points) and (12) (lines) from magnetization loops *5*, *4*, and *2* shown in Fig. 3b. (*1*) Critical current density for $P_a = 0$ and $H_{irr} = 200H_p$, (*2*) critical current density for $P_a = 0$ and $H_{irr} = 10H_p$, and (*3*) critical current density for $P_a = 0.3$ and $H_{irr} = 10H_p$.

and for a long plate with the rectangular cross section $2R \times w$,

$$J_{cm}(H) = \frac{2\Delta M(H)}{w(1 - w/3R)}, \quad (10b)$$

where ΔM is the magnetization loop width and $\Delta M = M^+(H) - M^-(H)$. However, this method gives incorrect results in the field range where there is an abrupt change in the critical current [29–31], for example, in the vicinity of $H = 0$. An alternative method for determining the dependence $J_{cm}(H)$ is the use of different analytical expressions for $j_c(B)$. The correspondence of the dependence $j_c(B)$ is judged from agreement between the calculated and experimental magnetization loops. The required dependence $J_{cm}(H)$ is obtained by replacing B with $\mu_0 H$ in formula (7) and by choosing the fitting parameters. For symmetric magnetization loops, the dependence $J_{cm}(H)$ expressed by function (7) coincides over the entire field range, except for weak fields H, with the curve obtained using formula (10). In this case, we have $l_s \ll R$, and the contribution from the equilibrium magnetization M_s is negligible. For a significant asymmetry of the magnetization loop, the values of J_{cm} obtained from formula (7) are much greater than those found using formula (10).

In the surface layer of the sample, the vortices are not pinned. Therefore, this layer is not involved in the supercurrent transport. This decrease in the effective cross section of the sample should be taken into account in the determination of the average (over the sample) critical current density. Thus, the dependence $J_{cm}(H)$ should include the decreasing function (7) and the change in the specific area of the core with the trapped magnetic flux:

$$J_{cm}(H) = j_c(H)S_{kern}(H)/S, \quad (11)$$

where S is the surface area of the sample (in the plane perpendicular to the field) and S_{kern} is the area of the central region with the pinned vortices. The quantity S_{kern} is zero for $H \geq H_{irr}$. The change in the area can be expressed through the depth of the surface layer:

$$J_{cm}(H) = j_c(H)(1 - l_s(H)/R)^n, \quad l_s < R,$$
$$J_{cm}(H) = 0, \quad l_s \geq R, \quad (12)$$

where $n = 2$ for a cylindrical sample and $n = 1$ for a thin plate. Figure 4 shows the dependences $J_{cm}(H)$ obtained using formulas (10a) and (12) from the magnetization loops shown in Fig. 3b, for different values of l_{s0}. For $l_s(H) \ll R$, the magnetization loop has a symmetric shape, and the curves obtained using formulas (10) and (12) coincide over the entire field range, except for weak fields H. The discrepancy between the curves $J_{cm}(H)$ obtained from formulas (10) and (12) increases with an increase in the surface layer depth l_s. The analytical relationship (12) successfully describes the behavior of the critical current density of the sample over the entire field range and agrees with the results presented in [29–31].

3. DISCUSSION

3.1. Applicability of the Model

The model under consideration is applicable primarily to homogeneous samples in the form of a long cylinder or plate, for which the magnetization loops are measured up to strong fields ($H_m \gg H_p$). The surface barrier [8] and demagnetization factor [32] are ignored in the described model, because their influence on the magnetization is small in fields exceeding H_p. It should be noted that the penetration of the magnetic flux into samples of other shapes [2, 16] occurs in much the same manner as for the distributions of the flux density B in Fig. 1.

In many cases, the magnetization loops of superconductors have a secondary peak (fishtail, peak-effect). Such loops can also be described in terms of the ECSM [19, 21, 22]. For this purpose, it is necessary to determine the function describing the peak in the dependence $j_c(B)$ and the corresponding dip in the dependence $l_s(H)$. The peak-effect is considered in detail in [33].

The ECSM can also be used to describe magnetization loops of inhomogeneous granular superconductors. In this case, the circulation radius of the screening current in the calculation will not coincide with the radius of the sample (see Subsection 3.2). In heterogeneous materials, the magnetization loop can have an additional diamagnetic contribution [17] (the loop

is rotated in the clockwise direction) or paramagnetic contribution [21, 22] (the loop is rotated in the counterclockwise direction). Also, the experimental dependence $M(H)$ can be a superposition of the magnetization loop of a superconductor and the loop of a ferromagnet [18]. In these cases, the magnetization of the sample is the sum of the magnetizations of each of the magnetic phases. For a qualitative parameterization, it is necessary to separate the contribution of the superconducting phase. Usually, the fraction of the superconducting phases can be judged from the change in the magnetization at temperatures above and below the critical temperature of the superconductor.

The grain size distribution function in the critical state model was taken into account in [3]. The simulation showed that, for the lognormal or Gaussian function of the grain size distribution, the shape of the magnetization loop remains qualitatively unchanged for different distribution parameters. The same conclusion was drawn in [34].

3.2. Scale of Circulation of the Screening Current

For granular superconductors, there is an ambiguity in choosing the size R, which determines the circulation region of the screening current [18, 35]. The size R can be chosen as the radius of the sample or as the effective radius of the grains. The supercurrent can also circulate in clusters consisting of several grains. In order to determine the critical current density from magnetic measurements, it is necessary to establish the scale of the circulation of the screening current, because the magnetization loop width is characterized by the parameter $P_w = j_{c0}R$. The asymmetry of the magnetization loop is characterized by the parameter $P_a = l_{s0}/R$; i.e., it also depends on the circulation radius of the supercurrent R. For the known magnetic field penetration depth λ_0, using the asymmetry parameter we can estimate the circulation scale of the screening current as $R \sim \lambda_0/P_a$. The value of λ_0 can be estimated using the London model for the reversible part of the magnetization loop. According to the London model [36], the equilibrium magnetization is described by the expression

$$M = -\frac{\varphi_0}{(32\pi^2\lambda_0^2)}\ln\left(\frac{\eta H_{c2}}{H}\right),$$

where φ_0 is the magnetic flux quantum and η is a constant of the order of unity.

For the analyzed granular superconductors [4, 7, 18, 20–22], the magnetization loops are successfully described by the ECSM (formulas (1)–(9)) with the effective grain radius as the value of R. The effective radius satisfying the fit is greater than or equal to the averaged grain radius determined from scanning electron microscopy images.

3.3. Parameterization

Let us list the main steps in the calculation of the magnetization loop of a superconductor.

1. If there is a contribution to the magnetization from nonsuperconducting phases, it is necessary to obtain the magnetization loop of the superconducting phase by filtering other contributions. In the obtained magnetization loop of the superconducting phase, the magnetization M must tend to zero with increasing field H up to H_{c2}.

2. The parameters of the superconductor λ, H_{irr}, and H_{c2} can be evaluated [37] and used in the fitting. The magnetic field H_{c2} is determined as a field in which the dependence $M(H)$ intersects with the H axis. The field H_{irr} is determined as the value of H above which the loop becomes reversible.

3. The dependence $l_s(H)$ (formula (8) or (9)) and the parameter $B_2 \sim 0.1\mu_0 H_{c2}$ are found from the estimated values of H_{irr} and H_{c2}.

4. The measured magnetization loop is used to construct the curve $\Delta M(H)$. This curve is fitted by relationship (12), which allows us to determine the parameter B_1.

5. The dependence $M(H)$ is calculated according to formulas (1)–(5) and (7) and then compared with the experimental loop. If the values of H_{irr} and H_{c2} were not determined previously, the parameters of the dependences $j_c(B)$ and $l_s(H)$ are chosen from the best fit of the calculated dependences and experimental magnetization loops. The main fitting parameters of the model $P_w = j_{c0}R$ and $P_a = l_{s0}/R$ determine the width of the magnetization loop along the M axis and its asymmetry relative to the H axis, respectively. The parameter P_w is comparable in order of magnitude with H_p (H_p and P_w exactly coincide for the field-independent current density $j_c(B) = j_{c0}$ [1]).

6. For granular superconductors, the circulation radius is estimated from the asymmetry of the loop ($R \sim \lambda_0/P_a$). The average grain size determined from scanning electron microscopy images can also be used. At the end, the value of $j_{c0} = P_w/R$ is determined.

4. CONCLUSIONS

In this paper, an extended critical state model was described. The model allows the calculation and parameterization of magnetization loops of type-II superconductors and takes into account the equilibrium magnetization of the surface layer. The asymmetry of the magnetization loop depends on the ratio of the surface layer depth to the sample size.

A new analytical expression was proposed for the dependence of the critical current density j_c on the magnetic field (7), which adequately describes the behavior of the critical current density j_c in weak and strong fields. It was established that the critical current

density depends on the size and shape of the sample, because the surface layer of the sample with a thickness ~ λ is not involved in the supercurrent transport.

The analysis of the ECSM, as applied to the parameterization of magnetization loops of polycrystalline superconductors, was carried out. In granular superconductors, the asymmetry of the magnetization loop makes it possible to determine the characteristic scale of circulation of the screening current and the bulk critical current density.

REFERENCES

1. C. P. Bean, Rev. Mod. Phys. **36**, 31 (1964).
2. D.-X. Chen, A. Sanchez, and J. S. Munoz, J. Appl. Phys. **67**, 3430 (1990).
3. V. V. Val'kov and B. P. Khrustalev, J. Exp. Theor. Phys. **80** (4), 680 (1995).
4. D. M. Gokhfeld, D. A. Balaev, S. I. Popkov, K. A. Shaykhutdinov, and M. I. Petrov, Physica C (Amsterdam) **434**, 135 (2006).
5. D.-X. Chen, R. B. Goldfarb, R. W. Cross, and A. Sanchez, Phys. Rev. B: Condens. Matter **48**, 6426 (1993).
6. D.-X. Chen, A. Hernando, F. Conde, J. Ramirez, J. M. González-Calbet, and M. Vallet, J. Appl. Phys. **75**, 2578 (1994).
7. D. M. Gokhfeld, D. A. Balaev, M. I. Petrov, S. I. Popkov, K. A. Shaykhutdinov, and V. V. Valkov, J. Appl. Phys. **109**, 033904 (2011).
8. D.-X. Chen, R. W. Cross, and A. Sanchez, Cryogenics **33** (7), 695 (1993).
9. L. Burlachkov, Phys. Rev. B: Condens. Matter **47**, 8056 (1993).
10. E. V. Blinov, R. Laiho, E. Lahderanta, Yu. P. Stepanov, K. B. Traito, and L. S. Vlasenko, J. Exp. Theor. Phys. **79** (3), 433 (1994).
11. X. Obradors and T. Puig, Supercond. Sci. Technol. **27**, 044003 (2014).
12. S. V. Yampolskii and Y. A. Genenko, Appl. Phys. Lett. **104**, 033501 (2014).
13. E. P. Krasnoperov, V. S. Korotkov, and A. A. Kartamyshev, J. Supercond. Novel Magn. **27**, 1845 (2014).
14. T. Schuster, H. Kuhn, E. H. Brandt, M. Indenbom, M. R. Koblischka, and M. Konczykowski, Phys. Rev. B: Condens. Matter **50**, 16684 (1994).
15. N. D. Kuz'michev and A. A. Fedchenko, Tech. Phys. **57** (5), 631 (2012).
16. M. Forsthuber and G. Hilscher, Phys. Rev. B: Condens. Matter **45**, 7996 (1992).
17. S. Altin and D. M. Gokhfeld, Physica C (Amsterdam) **471**, 217 (2011).
18. E. Altin, D. M. Gokhfeld, S. V. Komogortsev, S. Altin, and M. E. Yakinci, J. Mater. Sci.: Mater. Electron. **24**, 1341 (2013).
19. D. A. Balaev, D. M. Gokhfel'd, S. I. Popkov, K. A. Shaikhutdinov, L. A. Klinkova, L. N. Zherikhina, and A. M. Tsvokhrebov, J. Exp. Theor. Phys. **118** (1), 104 (2014).
20. Z. D. Yakinci, D. M. Gokhfeld, E. Altin, F. Kurt, S. Altin, S. Demirel, M. A. Aksan, and M. E. Yakinci, J. Mater. Sci.: Mater. Electron. **24**, 4790 (2013).
21. E. Altin, D. M. Gokhfeld, F. Kurt, and M. E. Yakinci, J. Mater. Sci.: Mater. Electron. **24**, 5075 (2013).
22. E. Altin, D. M. Gokhfeld, S. Demirel, E. Oz, F. Kurt, S. Altin, and M. E. Yakinci, J. Mater. Sci.: Mater. Electron. **25**, 1466 (2014).
23. M. I. Petrov, T. N. Tetyueva, L. I. Kveglis, A. A. Efremov, G. M. Zeer, K. A. Shaikhutdinov, D. A. Balaev, S. I. Popkov, and S. G. Ovchinnikov, Tech. Phys. Lett. **29** (12), 986 (2003).
24. P. W. Anderson and Y. B. Kim, Rev. Mod. Phys. **36**, 39 (1964).
25. A. S. Krasil'nikov, L. G. Mamsurova, N. G. Trusevich, L. G. Shcherbakova, and K. K. Pukhov, J. Exp. Theor. Phys. **82** (3), 542 (1996).
26. J. R. Clem, in *Low-Temperature Physics—LT14*, Ed. by M. Krusius and M. Vuorio (North-Holland, Amsterdam, The Netherlands, 1975), Vol. 2, p. 285.
27. R. Prozorov and R. W.Giannetta, Supercond. Sci. Technol. **19**, R41 (2006).
28. S. Senoussi, J. Phys. III **2**, 1041 (1992).
29. A. Tulapurkar, Phys. Rev. B: Condens. Matter **64**, 014508 (2001).
30. Y. Kimishima, M. Uehara, T. Kuramoto, Y. Ichiyanagi, Y. Iriyama, and K. Yorimasa, Physica C (Amsterdam) **377**, 196 (2002).
31. R. Lal, Physica C (Amsterdam) **470**, 281 (2010).
32. C. Navau and A. Sanchez, Supercond. Sci. Technol. **14,** 444 (2001).
33. D. M. Gokhfeld, J. Supercond. Novel Magn. **26**, 281 (2013).
34. Q. Hong and J. H. Wang, Appl. Supercond. **2**, 697 (1994).
35. J. Horvat, S. Soltanian, A. V. Pan, and X. L. Wang, J. Appl. Phys. **96**, 4342 (2004).
36. Z. Hao and J. R. Clem, Phys. Rev. Lett. **67**, 2371 (1991).
37. I. L. Landau, J. B. Willems, and J. Hulliger, J. Phys.: Condens. Matter **20**, 095222 (2008).

Translated by O. Borovik-Romanova